

ANALYSIS METHOD FOR NON-NOMINAL FIRST ACQUISITION

Detlef Sieg⁽¹⁾,
Roberta Mugellesi-Dow⁽²⁾

⁽¹⁾EDS Operations Services GmbH at ESA/ESOC
Robert-Bosch-Straße 5, D-64293 Darmstadt (Germany)
Detlef.Sieg@eds.com

⁽²⁾ESA/ESOC,
Robert-Bosch-Straße 5, D-64293 Darmstadt (Germany)
Roberta.Mugellesi.Dow@esa.int

Abstract: First this paper describes a method how the trajectory of the launcher can be modelled for the contingency analysis without having much information about the launch vehicle itself. From a dense sequence of state vectors a velocity profile is derived which is sufficiently accurate to enable the Flight Dynamics Team to integrate parts of the launcher trajectory on its own and to simulate contingency cases by modifying the velocity profile. Then the paper focuses on the thorough visibility analysis which has to follow the contingency case or burn performance simulations. In the ideal case it is possible to identify a ground station which is able to acquire the satellite independent from the burn performance. The correlations between the burn performance and the pointing at subsequent ground stations are derived with the aim of establishing simple guidelines which can be applied quickly and which significantly improve the chance of acquisition at subsequent ground stations. In the paper the method is applied to the Soyuz/Fregat launch with the MetOp satellite. Overall the paper shows that the launcher trajectory modelling with the simulation of contingency cases in connection with a ground station visibility analysis leads to a proper selection of ground stations and acquisition methods. In the MetOp case this ensured successful contact of all ground stations during the first hour after separation without having to rely on any early orbit determination result or state vector update.

1. INTRODUCTION

The first acquisition of a satellite relies on the separation element dispersion values as they are given in the Interface Control Document issued by the launcher authority. This does not cover those cases in which the satellite is delivered into a non-nominal orbit due to a launcher failure. As this paper shows for an example with the MetOp-A satellite, a proper analysis before the launch can enable the Flight Dynamics Team even in such contingency cases to support a successful initial acquisition. This is especially important since sometimes the scheduled delivery times of updated separation elements can be missed or late. There have been launches where the officials communicated a misperformance or even a complete launcher failure only after the nominal acquisition times of several ground stations.

2. STEPS OF ANALYSIS

The chance of S/C acquisition during the first nominal contact period of each ground station can be significantly increased by a simulation of the most likely contingency cases and a proper analysis of the resulting trajectories and ground station pointing.

As a first step this requires analysis of the launch vehicle trajectory and modelling of some parts of it in a way that allows the simulation of an underperforming thrust level

with the goal of getting sets of separation elements with respect to the launcher performance.

In some cases the mission might be lost in the sense that it might no longer be possible to reach an orbit which allows to fulfil at least some of the mission goals.

As second step the subsequent influence on the ground station pointing can be analysed with the aim of identifying ground stations and acquisition methods such that the satellite can be acquired for most or all possible trajectories. The ground station might have to be prepared for an earlier or later acquisition and to start searches at the most efficient times.

Further analysis work can be done which would enable the Flight Dynamics Expert to draw conclusions as soon as the S/C is acquired by one ground station. Then, only a few obtained pointing values are needed together with the analysis results to give quickly clear guidelines to the following stations. These include the provision of time offset values (TOV) and start times for searches.

Specific examples for this will be shown from the analysis performed for the MetOp-A launch in 2006.

Finally procedures should be derived and tested together with the Flight Control Team and ground station personnel. For the MetOp-A launch an extensive training was done during the simulation campaign which included several simulated non-nominal launches.

3. LAUNCHER TRAJECTORY MODELLING

3.1 General aspects

For the modelling of the launcher trajectory it is advantageous if the flight profile of the launcher does not depend on the launch date or time which means it is fixed relative to the Earth. This is often the case for launches into Earth bound orbits. Then the launcher trajectory modelling needs to be done only once.

The dispersion values provided together with the separation elements cover only the 3σ -injection accuracy in case of a nominal behaviour of the launcher. Usually there is no information available about contingency cases. In case of occurrence some of them can be covered on the basis of own assumptions or better experiences gained during earlier launches.

The only information provided in addition to the separation elements is typically a sequence of state vectors describing the nominal ascent path of the launcher. An extract of such a sequence is given in Table 1. The time counts in seconds from liftoff. Such a table is the basis for the whole analysis.

Often the trajectory is given in a certain launch pad system or an Earth fixed system which is frozen at lift off, i.e. the Earth rotation around the z-axis stops at lift off to get an approximately inertial coordinate system. The state vectors in Table 1 are given in Greenwich coordinate system, frozen at lift-off. In this case as a first step all state vectors are converted to the same system which is used for the satellite trajectory integration after separation.

Then the state vector sequence can be converted to an impulsive velocity profile as shown in Table 2 as follows.

For each state vector perform a free drift integration to the next state vector and compare the velocity components. As a first guess put the velocity difference as an impulsive manoeuvre at the midpoint of the current integration interval and repeat the integration. The modelling of the acceleration by one impulsive Δv at the midpoint of the current integration interval leads to a small position error at the end of the integration interval. This error can be compensated by two manoeuvres: One at the start and one at the end of the interval. The position correction is achieved through dividing the required correction by the time interval and putting the calculated Δv as first manoeuvre and the opposite Δv as second manoeuvre. Then all calculations are improved iteratively by repeating the integration and modelling of the remaining velocity and position discrepancy in the same way.

As the last impulsive Δv of the current interval is at the same time as the first impulsive Δv of the next interval these two manoeuvres are just combined to one. In the example the orbit integration was done in the inertial J2000 coordinate system without airdrag. The error due

Table 1. Launcher profile as state vectors

t [s]	x[km]	y[km]	z[km]
	v_x [m/s]	v_y [m/s]	v_z [m/s]
944.11	1053.866	100.959	6457.083
	-1915.146	-7413.309	336.312
954.11	1034.612	26.674	6460.042
	-1935.689	-7443.574	255.399
964.11	1015.153	-47.911	6462.189
	-1956.200	-7473.305	173.770
974.11	995.488	-122.790	6463.515
	-1976.678	-7502.489	91.419
984.11	975.619	-197.959	6464.015
	-1997.120	-7531.111	8.341
994.11	955.546	-273.410	6463.680
	-2017.522	-7559.158	-75.469
1004.11	935.269	-349.140	6462.503
	-2037.881	-7586.615	-160.015

Table 2. Launcher trajectory as Δv profile

t [s]	x[km]	y[km]	z[km]
944.11	-0.06109	-0.01078	-0.04266
949.11	12.77387	27.05895	10.73802
954.11	-0.02579	0.00864	0.07187
959.11	13.13002	27.50460	10.09287
964.11	0.08817	-0.08138	-0.10910
969.11	13.48667	27.94182	9.42735
974.11	-0.03457	0.10883	0.11543
979.11	13.84135	28.36900	8.74223
984.11	-0.05428	-0.12487	-0.05505
989.11	14.19352	28.78817	8.03715
994.11	0.05500	0.13890	-0.02101
999.11	14.54361	29.19691	7.31285

to this is also compensated by the position correction manoeuvres. The obtained velocity profile is suitable for the further analysis as long as the position correction manoeuvres have a small size compared to the main impulsive manoeuvres modelling the launcher acceleration. The main manoeuvres are marked in bold style in Table 2. The size of the other corrective manoeuvres is less than 1% in magnitude compared to the main manoeuvres.

The position correction manoeuvres do not have a real physical meaning. They are “misused” to model discrepancies between the trajectory modelling by the launcher operating authority and the trajectory modelling by the satellite orbit integrator. However they ensure that precise separation elements are achieved by performing one single orbit integration through the velocity profile.

Now contingencies of the thrust level or burn duration can be simulated by cutting the velocity profile at a certain time or by multiplying all Δv -pulses during a certain interval with a performance factor followed by a re-integration of the whole trajectory.

3.2 Example Artemis

Artemis is a telecommunications satellite with new, advanced technologies that expands and improves all areas of navigation, mobile communication and satellite to satellite communications. Artemis was launched in the year 2001 with the Ariane-5 flight 142. However the planned geostationary transfer orbit was not reached as can be seen from Table 3.

Table 3. Injection parameters Ariane flight 142¹

Parameter	Actual	Target
perigee	592 km	858 km
apogee	17528 km	35786 km
inclination	2.9 deg	2 deg
argument of perigee	153 deg	178 deg

Level-0 telemetry analysis showed that the solid boosters and the main stage engine functioned correctly. The thrust delivered by the upper-stage engine, however was not sufficient to allow correct injection of the satellite into GTO.

The actual separation elements of this case could be reproduced quite well from the ascent trajectory velocity profile assuming 80% performance throughout the burn of the upper-stage. This example shows that a velocity profile can indeed be used to model a real contingency case.

Thanks to its ion propulsion system Artemis was still able to reach its geostationary orbit although one year later than originally planned.

3.3 MetOp-A

The Meteorological Operational satellite programme (MetOp) is a new European undertaking providing weather data services that will be used to monitor climate and improve weather forecasts. The MetOp programmes series of three satellites has been jointly established by ESA and the European Organisation for the Exploitation of Meteorological Satellites (EUMETSAT), forming the space segment of EUMETSAT's Polar System (EPS).

The launch and early orbit phase operations were conducted by ESOC on behalf of EUMETSAT.

1. Ariane launcher programme board, *Report on Flight 142*, ESA/PB-ARIANE(1001)90, Paris, 26 July 2001

For MetOp a launcher velocity profile was calculated to analyse the ground station visibility during the first orbit after launch to assess the problems related to the first acquisition at Kerguelen, Malindi, Kiruna, Alaska and Hawaii and to identify a procedure to be followed to ensure a successful acquisition under non/nominal circumstances. Baseline for the analysis was a launch on 30.Jun.2006 whereas the actual launch of MetOp took place on 19.Oct.2006 with an identical trajectory relative to the Earth. The launch occurred from the Baikonur Cosmodrom with a Soyuz rocket equipped with a Fregat upper stage. The lower composite consists of four boosters (first stage), a core (second) stage and a third stage. On top of the third stage an interstage section connects the restartable Fregat upper stage followed by spacecraft adapter and MetOp. Fregat and MetOp were secured by the payload fairing.

The first three stages use a standard ascent trajectory. The first stage provides the highest thrust level. The boosters burn for 118 seconds and are then discarded. The second stage is equipped with one RD-108A engine and four vernier thrusters for three-axis flight control. The second stage burns for 290 seconds. The third stage is equipped with one RD-0110 engine and four vernier thrusters that handle attitude control of the vehicle. After separation of the Fregat/MetOp composite from the launch vehicle a **first Fregat burn** ($\Delta v = 1296$ m/s) follows immediately to inject the composite from the sub-orbital trajectory (fictitious perigee height of -2300 km) to the transfer orbit with an apogee of $H_a = 850.4$ km.

The **second Fregat burn** ($\Delta v = 181$ m/s) to raise the perigee of the transfer orbit and to reach the separation orbit (see Table 4) occurs half a revolution later at apogee.

Table 4. Separation elements for launch on 2006/06/30

	Transfer orbit after 1st Fregat burn	Separation orbit after 2nd Fregat burn
t	0h:17min	1h:04min
a	6859 km	7189 km
e	0.04676	0.002427
i	98.73 deg	98.74 deg
Ω	241.01 deg	241.05 deg
ω	94.13 deg	108.58 deg

In the MetOp case the launcher trajectory modelling has been restricted to the two Fregat burns as anyway the Δv of all three Soyuz stages and more than 80% of the first Fregat burn are needed to reach an orbit around the Earth. Furthermore the Fregat upper stage has an independent digital control system with a three-axis gimballed IMU. The system is able to correct errors introduced by the Soyuz control system. This was demonstrated during the

second Cluster-II launch, where an underperformance of the third stage of the Soyuz rocket was compensated by performing a non-nominal longer or stronger 1st Fregat burn such that the sum of Soyuz third stage + 1st Fregat burn was almost nominal. However the second burn was shorter as Fregat run out of fuel. An underperformance of the third Soyuz stage can therefore be simulated to a large extent by an earlier ending burn of Fregat.

The Fregat trajectory profile was supplied by the launcher authority via fax¹ as a sequence of state vectors, one every 10 second during the burns and one every 60 seconds otherwise. In fact Table 1 gives an extract of this. The sequence of state vectors has been converted to a velocity profile as already explained in section 3.1.

Finally a velocity profile from liftoff + 530s till liftoff + 1h:09min was available which could be used for further contingency and ground station visibility analysis as described in section 5.

4. STANDARD ACQUISITION METHODS

The standard for station predictions at ESA stations are STDM files (Spacecraft Trajectory Data Messages). They contain a sequence of Earth-fixed state vectors. The pointing direction is calculated at the station by means of a piecewise cubic Hermite interpolation and a subsequent transformation into the topocentric system. Providing not only one but a sequence of state vectors has the advantage that the station can follow powered flight trajectories as long as the supplied state vector sequence is dense enough during manoeuvres. The advantage of using the Earth-fixed system instead of using a topocentric system or direct provision of pointing values is that the STDM file does not depend on the location of the ground station and therefore the same file can be used by all ground stations.

Two standard methods, which can be combined, are supported by most ground stations to ease the acquisition in case the satellite deviates from the nominal trajectory: The first method is a circular search around the nominal trajectory. More details are given in [1].

The second method is the application of a Time Offset Value (TOV).

The application of a TOV is most effective if a satellite is almost on the nominal trajectory with a delay as it is the case if along track shifts accumulate for near Earth satellites due to fluctuations of the air drag. In this case the TOV observed during the last pass is always a good initial guess for the next pass as long as the ground station predictions are not updated.

A simple way to define a TOV would be to base the value only on the pointing evolution of one antenna axis, e.g.

¹Fax ST/DE-DT/217/06/LF/lf from Starsem on 2006/06/02

the secondary antenna axis, i.e. the elevation in most cases. Then the TOV is the time delay till a certain nominal elevation value is reached. However this definition is no longer applicable when the elevation changes slowly around the maximum value.

The better definition of the TOV is that the overall pointing deviation is minimized. This means recording of the antenna pointing at a certain epoch t_0 , while the antenna is in autotrack mode. The pointing is then transformed into a direction vector in the topocentric system at t_0 . This vector is then compared with the predicted direction vector for the same epoch by calculating the angular difference between the two. Subsequently this angular difference is minimized by varying the time at which the nominal pointing direction is calculated. When calculating the direction vector from pointing values at a time t one has to be aware that these values refer to the topocentric coordinate system at t . Due to the rotation of the Earth the topocentric coordinate systems at t_0 and t have a different orientation with respect to the inertial system. Often this difference is neglected since the error due to this is small if the satellite movement dominates the Earth rotation and the TOV values are reasonable small. The corresponding error is illustrated in Fig. 1.

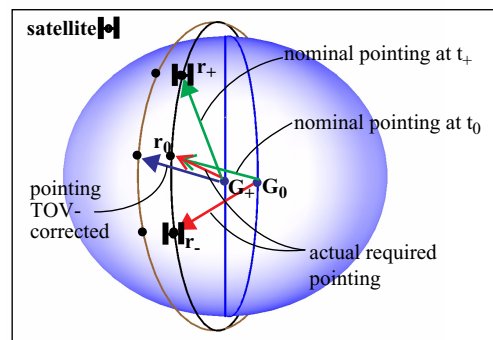


Fig. 1. TOV correction without Earth rotation

The nominal satellite orbit is drawn in black (circle with the satellite symbols). Assume that the satellite is delayed by Δt compared to the nominal track and that the satellite reaches nominally the positions r_- , r_0 and r_+ at the times $t_- = t_0 - \Delta t$, t_0 and $t_+ = t_0 + \Delta t$. Then the actual required pointing at t_+ and t_0 is given by the red arrows whereas the nominal pointing is given by the green arrows. The ground station location G on Earth is shown at t_0 and $t_0 + \Delta t$ and is labelled by G_0 and G_+ . If now the ground station applies a TOV of size $-\Delta t$ but still refers the pointing to the topocentric system defined by itself, i.e. neglecting the Earth rotation during Δt , then this corresponds to a satellite trajectory shifted (better rotated) to the left and the ground station points along the blue arrow labelled as TOV corrected. This is much closer to the actual pointing but still deviates slightly.

All TOVs and associated pointing deviations in the following sections have been derived under the assumption that the Earth rotation is not considered by the

ground station when applying the TOV.

An example of a typical improvement of the pointing by the application of certain time offset values is given in Fig. 2. One fixed TOV is applied throughout the complete pass and the obtained depointing is shown for different TOVs. In Fig. 2 the minimal depointing is achieved with a TOV of 28 seconds. The other curves show the depointing for TOVs between 16 and 40 seconds which means an TOV up to 12 second smaller or larger.

Looking only at the three best cases (TOV=25s, 28s or 31s) in Fig. 3 one sees that the best pointing at the beginning of the pass is achieved with the smaller TOV of 25 seconds whereas the best TOV at the end of the pass would be 31s (here best means smallest depointing). Nevertheless the TOV of 28 seconds is a good compromise throughout the whole pass as it is not more than 0.2 degree away from the best possibility.

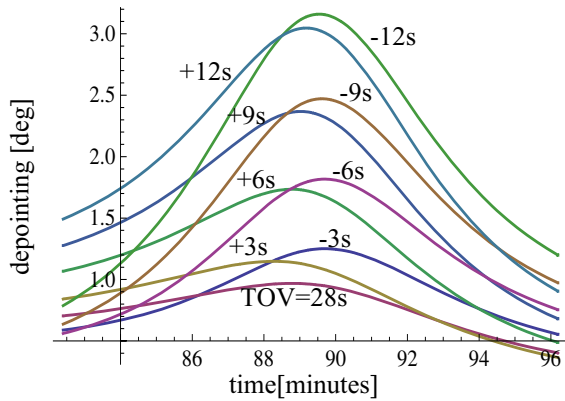


Fig. 2. Depointing improvement by TOV correction

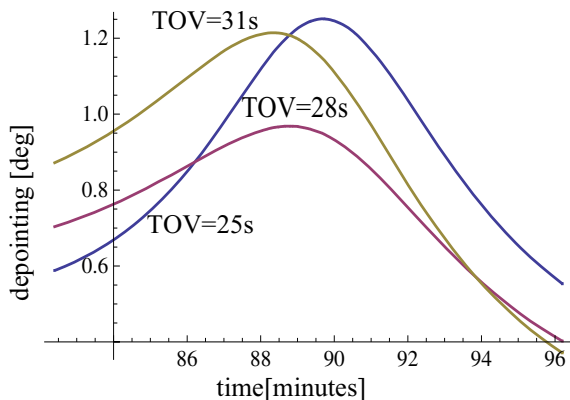


Fig. 3. Depointing improvement by TOV correction

This must not always be like this especially during long passes. However in the following analysis it was always very similar to the shown situation and therefore only one TOV value is given for every pass in the following MetOp analysis.

5. ANALYSIS METOP

Before proceeding with the contingency analysis it shall not be forgotten to mention that the actual launch of MetOp was very nominal with an position deviation at separation of only 7 km or the following differences of the elements: $\Delta a = 5 \text{ km}$, $\Delta e = 0.00013$, $\Delta i = 0.005 \text{ deg}$, $\Delta \Omega = 0.05 \text{ deg}$, $\Delta(\omega + \nu) = 0.05 \text{ deg}$. Therefore at the end procedures based on the contingency analysis were not needed during actual operations.

5.1 Contingency Analysis Assumptions

Using the derived velocity profile of Fregat (see section 3.3) the following two major cases have been analysed.

Case 1: Non-nominal first Fregat burn followed by a nominal second Fregat burn.

Case 2: Nominal first Fregat burn followed by a non-nominal second Fregat burn.

For the case of a non-nominal first burn followed by a non-nominal second Fregat burn it is assumed that at least for small errors the two single errors can be superimposed.

Concerning the first case it has to be noted that the satellite cannot be delivered into an orbit if more than 20% of the nominal Δv are not provided, which corresponds to a shortening of the burn of 60 seconds. Therefore the maximal performance error considered in the visibility analysis is -15% which correspond to a remaining perigee height of 200 km. Two different kinds of contingencies were simulated.

- In the subcase 1A, the Δv has been removed throughout the profile by applying a performance factor to the whole Δv -profile. This corresponds to an engine performance problem during the burn. It is assumed that the pointing of the composite is still nominal, i.e. it is kept as in the original velocity profile.
- In the subcase 1B, the Δv has been removed at the end of the burn corresponding to a premature engine cut-off.

It turned out that the resulting inclination and ascending node are not effected by both simulated performance problems. The influence on the shape of the orbit is very similar in both cases. The ratio of semi major axis to eccentricity is modified in the same way, however the absolute change of the semi major axis is 10% higher in subcase 1A. Concerning the position within the orbit, i.e. argument of perigee plus true anomaly, the difference between 1A and 1B is only 0.4 degree in the worst case whereas the deviation from the nominal separation elements is 18 degree.

As both cases are quite similar only the results from the subcase 1A are given in the following section. The same applies to case 2 where the burn is much shorter in magnitude and duration.

No simulations have been performed for a non-nominal attitude of Fregat.

5.2 Fregat/MetOp ground track

The ground track of Fregat and the first MetOp orbit is shown in Fig. 4. The Fregat ground track is drawn in blue and the location of the two burns is shown. After separation the MetOp ground track is shown in red. Amongst others the following five ground stations were identified which have satellite visibility after separation: Kerguelen (Indian Ocean, French), Malindi (Kenia), Kiruna (Sweden), North Pole (Alaska) and South Point (Hawaii). Kerguelen is operated by le Centre national d'études spatiales (CNES), the government agency responsible for shaping and implementing France's space policy in Europe. Malinda and Kiruna are part of ESTRACK, the ESA tracking network. North Pole and South Point belong to PioraNet, operated in partnership between the Swedish Space Corporation and the USA company Universal Space Network. The visibility areas covered by these ground stations are shown in green. They are valid for a nominal height of MetOp of about 800 km.

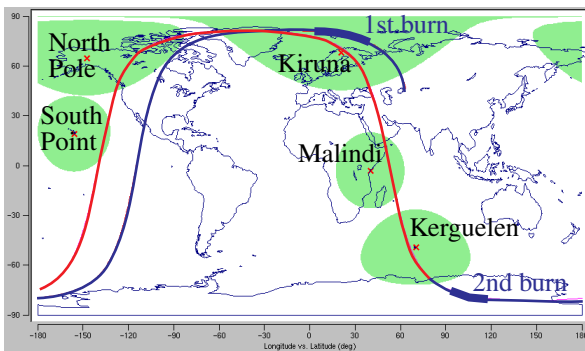


Fig. 4. Fregat and MetOp ground track

One major thing to notice is that all ground stations which are used by the launcher authority to track Fregat are on Russian territory. There is no visibility between end of 1st Fregat burn and separation. The visibility of the Russian station Narian-Mar ended more than 2 minutes before the end of the 1st burn. Therefore the only available data from the launcher authority before MetOp acquisition at Kerguelen and Malindi could be Fregat telemetry from 2/3 of the first burn, but no radiometric data for an updated orbit determination afterwards and no information at all about the second burn, which makes the overall analysis even more important.

Additionally the situation was improved by a collaboration with United States Strategic Command's (USSTRATCOM). Space surveillance is a critical part of their tasks which involves detecting, tracking, cataloguing and identifying man-made objects orbiting the Earth. For this they operate the Space Surveillance Network of radar stations. Based on provided nominal trajectory data they used some of their stations in North America to observe Fregat after the 1st burn. From acquisition and loss of signal times a first conclusion on the performance of the first burn could be drawn supplemental to the following observations at Kerguelen.

5.3 Visibility analysis

Based on the contingency cases 1 and 2 the visibility analysis was performed for the five ground stations Kerguelen, Malindi, Kiruna, Alaska and Hawaii. The visibility analysis consists of five basic plots for each ground station and contingency case plus additional TOV-improved depointing plots where applicable. In the following sections an extract of the plots and the associated conclusions are given for Kerguelen, Malindi and Kiruna. Information about the other stations is available in the technical note¹.

5.3.1 Kerguelen

In Fig. 5 to Fig. 9 the basic plots for Kerguelen and the 1st Fregat burn are shown.

The nominal evolution of azimuth and elevation over time is shown together with the evolution in case of a performance variation between -15% and +2% of the first burn (Fig. 5 and Fig. 6).

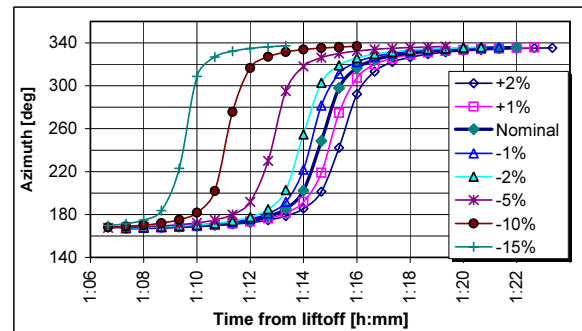


Fig. 5. Azimuth at Kerguelen, 1st burn

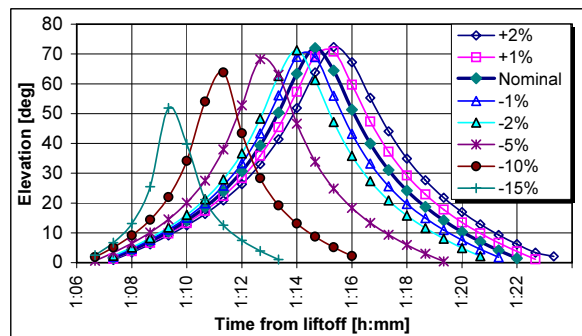


Fig. 6. Elevation at Kerguelen, 1st burn

As a next step the differences between the non-nominal and the nominal values are calculated and shown in the Δ azimuth and Δ elevation plots in Fig. 7 and Fig. 8.

1. Mugellesi, R.; Sieg, D., *MetOp-A Initial Station Acquisition*, ESA/ESOC Technical Note, EPS-FDOS-OD-TN-0001-OPS-GFM, Darmstadt, Germany, 2006

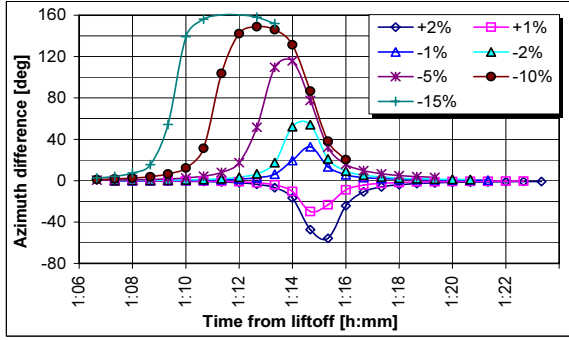


Fig. 7. Δ Azimuth at Kerguelen, 1st burn

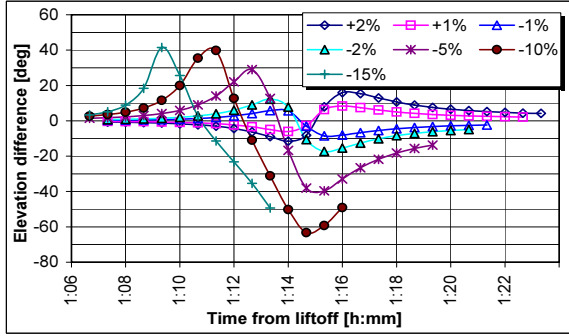


Fig. 8. Δ Elevation at Kerguelen, 1st burn

More important for the acquisition of the signal is the overall depointing as shown in Fig. 9. It is calculated from corresponding pairs of pointing vectors. It can also be calculated approximately with equation 1.

$$\Delta p = \sqrt{(\Delta az \cdot \cos el)^2 + \Delta el^2} \quad (1)$$

where:

Δp is the depointing angle.

Δaz , Δel are azimuth and elevation difference.

el is the elevation.

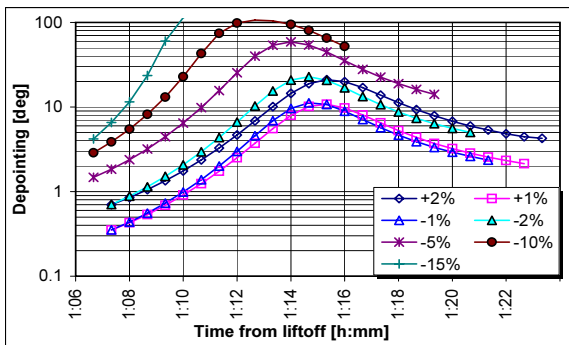


Fig. 9. Depointing at Kerguelen, 1st burn

For the 2nd burn the whole performance range between 0 and 100% was analysed and the evolution of Δ azimuth, Δ elevation and the whole depointing are shown for three different performance factors corresponding to 20%, 50% and 100% (=no burn) underperformance in Fig. 10 to Fig. 12.

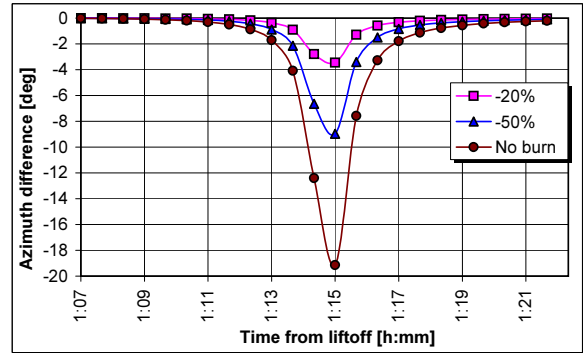


Fig. 10. Δ Azimuth at Kerguelen, 2nd burn

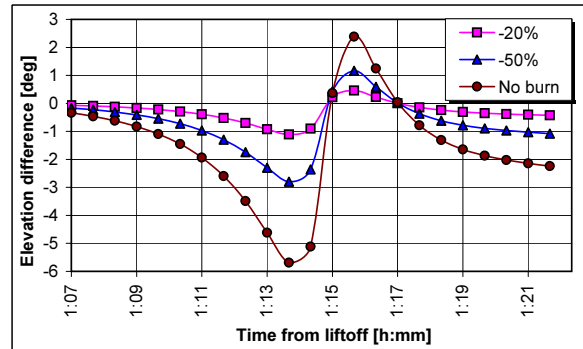


Fig. 11. Δ Elevation at Kerguelen, 2nd burn

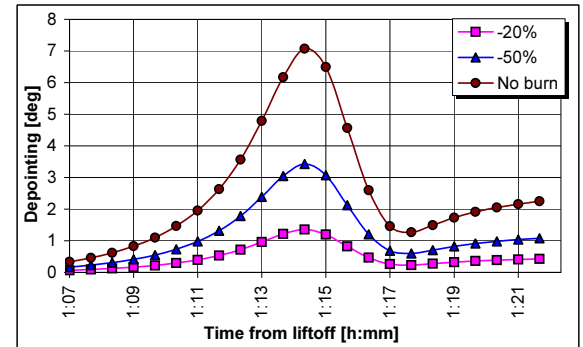


Fig. 12. Depointing at Kerguelen, 2nd burn

Looking through the Kerguelen plots the following conclusions can be drawn:

- Fig. 6: The 5 deg elevation crossing is up to one minute earlier.
- As the pass of Kerguelen starts shortly after end of the second Fregat burn, elevation and azimuth are less sensitive to the 2nd burn performance than during subsequent ground station contact periods. (e.g. compare Fig. 12 and Fig. 20).
- The small antenna at Kerguelen has a beamwidth of 5 degrees. It can acquire the spacecraft in all given contingency cases as the maximal depointing at the beginning of the pass is 3 degrees in case 1 (Fig. 9) and much below 1 degree in case 2 (Fig. 12). In case of a moderate performance error during the first burn the satellite can be acquired during several minutes for any performance error due to the second burn.

- The elevation difference due to a misperformance of the second burn is rather low around 1:15 and at 1:17 (Fig. 11) whereas due the 1st burn an offset between 5 and 50 degrees would be observed (Fig. 8). From the reported elevation values at these times a quick conclusion could be drawn on the performance of the first burn.
- The influence of a moderate performance error (some percent) of the second burn on the pointing can be neglected as 20% performance error correspond to a maximal depointing of 1.1 degree (Fig. 12).

5.3.2 Malindi

For Malindi plots of the elevation depending on the 1st burn performance (Fig. 13) and plots of the depointing depending on 1st (Fig. 14) and 2nd burn (Fig. 16) performance are given.

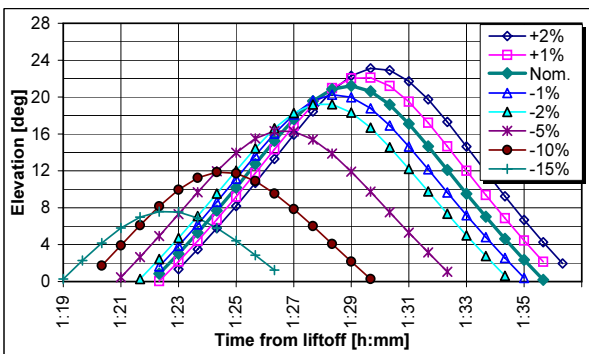


Fig. 13. Elevation at Malindi, 1st burn

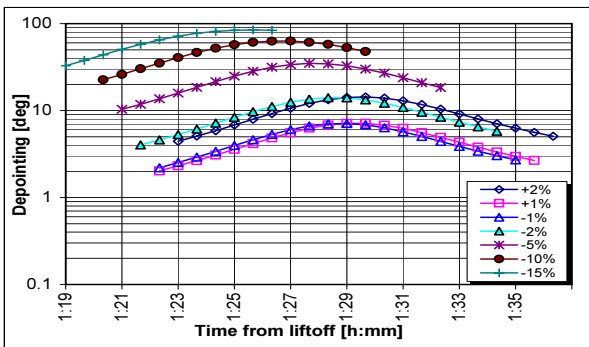


Fig. 14. Depointing at Malindi, 1st burn

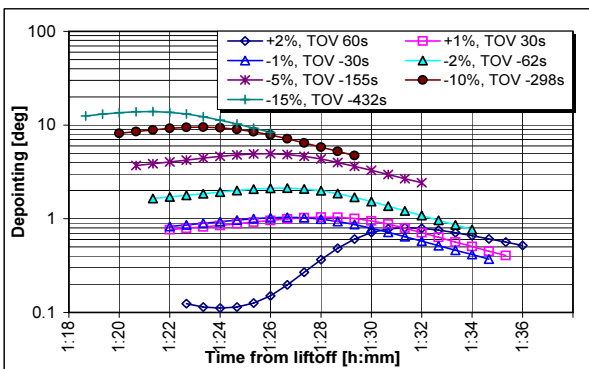


Fig. 15. TOV improved depointing at Malindi, 1st burn

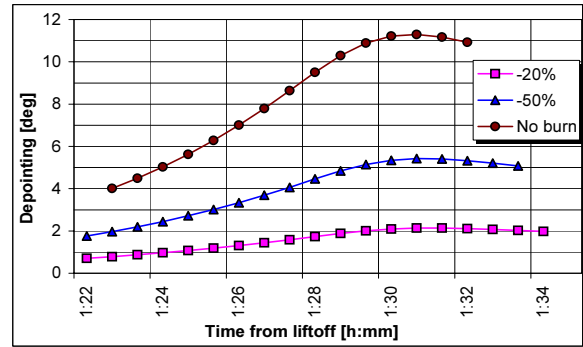


Fig. 16. Depointing at Malindi, 2nd burn

A new type of plot is Fig. 15. It shows how the depointing due to the first burn can be reduced if certain TOVs are applied which depend on the burn performance. As a reasonable guess of the burn performance was already possible during the previous Kerguelen pass, the corresponding TOV can be applied at Malindi to improve the pointing.

Looking through the Malindi plots the following conclusions can be drawn:

- Fig. 13: The 4 deg elevation crossing is up to three minutes earlier.
- Although the maximal reached elevation (Fig. 13) depends significantly on the burn performance, the depointing can be reduced significantly if the initial guess of the performance error from Kerguelen is used to apply the corresponding TOV at Malindi. Compare Fig. 14 and Fig. 15: For example in the two percent underperformance case the maximal depointing is reduced from more than 10 to 2 degree. If only the first burn misperformed the satellite could still be acquired by a circular search during the second half of the pass where the maximal depointing decreases below 5 degree for the -10% case (Fig. 14). (A five degree cone around the nominal trajectory could be scanned within a few minutes).
- If only the second burn has a misperformance the satellite can be acquired with a circular search at the beginning of the pass where the depointing is below 5 degree for all performances (Fig. 16).
- The observed depointing during the second half of the pass can give a good clue on the performance of the second burn in case of a moderate performance error of the first burn and a compensation of 1st burn errors by a TOV.
- The time shift of loss of signal can give a confirmation of the first burn performance.
- The influence of a moderate performance error (some percent) of the second burn on the pointing can be neglected as 20% performance error are required to reach 2% depointing.

5.3.3 Kiruna

For Kiruna the same type of plots are shown as for Malindi. These are for a varying first burn performance the elevation plot (Fig. 17), the depointing plot (Fig. 18) and the TOV improved depointing (Fig. 19). For a varying second burn performance the depointing plot is given in Fig. 20.

Looking through the Kiruna plots the following conclusions can be drawn:

- The 10 deg elevation crossing is up to eight minutes earlier (Fig. 17).
- The performance of the first burn has only a very minor influence on the maximal reached elevation of about 70 degree (Fig. 17). This is completely different to Malindi (Fig. 13) and one prerequisite to get such an extraordinary reduction of the pointing error when applying a TOV as shown in Fig. 19. Of course a guess of the first burn performance during previous stations is required for this.
- If the pointing error of the first burn is compensated by a TOV (or was nominal) then in most cases an acquisition is possible with a search at the beginning of the pass. (Only few degrees depointing in Fig. 19 and Fig. 20).
- The depointing during the middle of the pass can give a good indication of the second burn performance (Fig. 20).

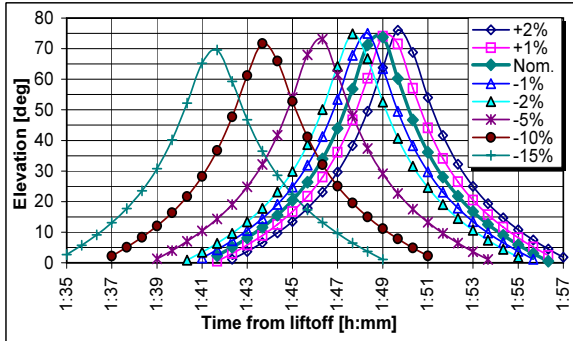


Fig. 17. Elevation at Kiruna, 1st burn

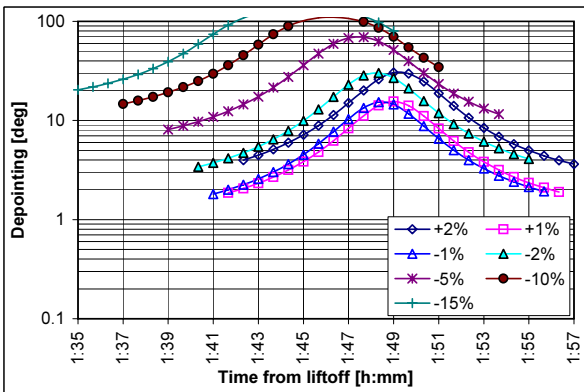


Fig. 18. Depointing at Kiruna, 1st burn

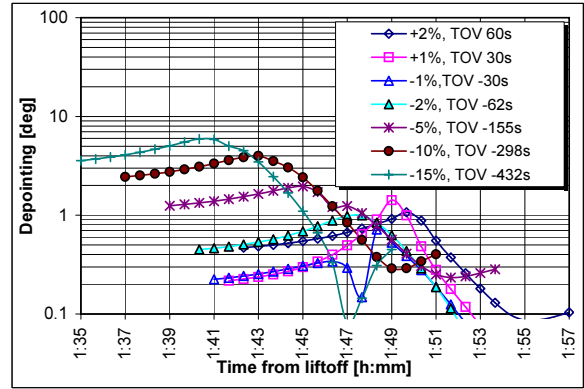


Fig. 19. TOV improved depointing at Kiruna, 1st burn

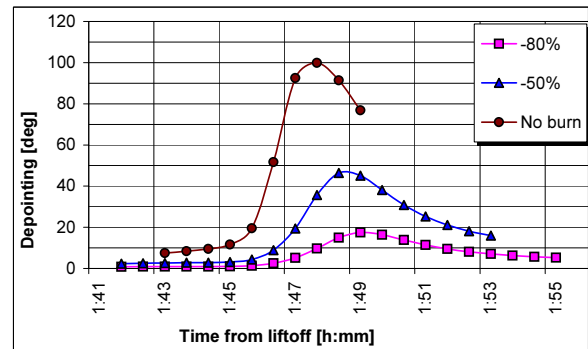


Fig. 20. Depointing at Kiruna, 2nd burn

5.3.4 Applicability of TOV correction

So far the obtained results have shown that a TOV correction can improve the depointing a lot even in cases of major differences of the trajectory due to a launcher contingency. A complete overview of the obtained values with respect to the performance of the first burn is given in Table 5.

Table 5. TOV at ground stations

	Performance of 1st Fregat burn						
	-15%	-10%	-5%	-2%	-1%	+1%	+2%
Kerguelen	-	-	-	-	-	-	-
Malindi	-432s	-298s	-155s	-62s	-30s	+30s	+60s
Kiruna	-432s	-298s	-155s	-62s	-30s	+30s	+60s
Alaska	-430s	-290s	-150s	-60s	-30s	+30s	+60s
Hawai	-	-	-	-	-	-	-

However this is not the case all along the trajectory and for all ground stations. We saw already that for some stations the maximum elevation values vary a lot depending on performance, however on a different station not. It is also surprising to see that in this analysis the TOV is not growing in between the three ground stations Malindi, Kiruna and Alaska. Only a proper analysis in advance helps to draw the correct conclusions quickly.

Of course the geometry can also be such that a TOV correction is not applicable at all. An example for this is the change of visibility due to different performances of the second burn at Malindi. Plots of elevation, azimuth and Δ azimuth are given in Fig. 21 to Fig. 23.

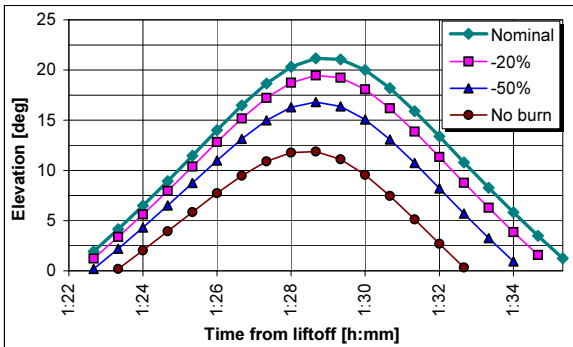


Fig. 21. Elevation at Malindi, 2nd burn

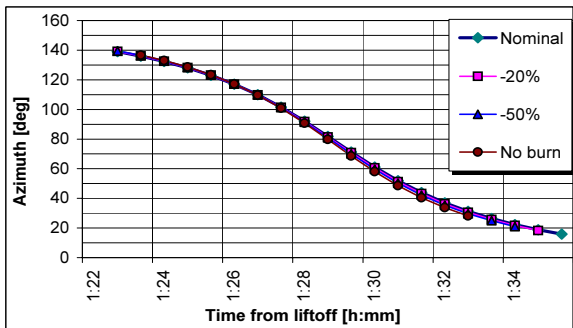


Fig. 22. Azimuth at Malindi, 2nd burn

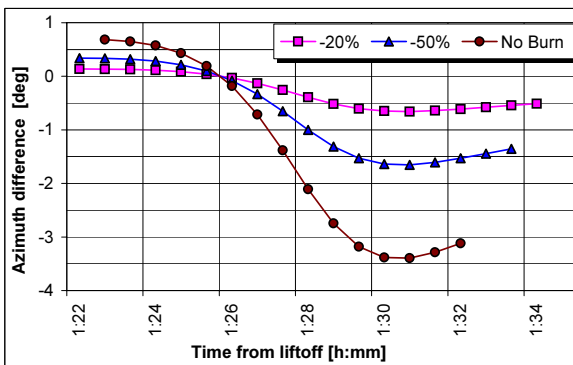


Fig. 23. Δ Azimuth at Malindi, 2nd burn

Already the elevation plot (Fig. 21) shows that only a varying TOV could compensate the elevation change as one would have to shift the non-nominal curve towards the left at the beginning of the pass and to the right at the end of the pass to make it coincide with the nominal one. The required shift would be in the order of 1-2 minutes for the 50% curve (the blue one with triangles). However without any TOV the values of Δ azimuth (Fig. 23) are rather small throughout the pass. Shifting the azimuth curve in Fig. 22 by 1-2 minutes would result in an azimuth deviation of more than 10 degrees and therefore the overall pointing would only deteriorate in case of applying a TOV.

6. CONCLUSIONS

It has been shown that performance related contingency cases of the launcher can be simulated by the modelling of the trajectory as velocity change profile. This method can be applied to all launches where the nominal launcher trajectory is available as a sequence of state vectors. At ESOC this has been done already for Ariane, Proton and Soyuz/Fregat launches. For Soyuz/Fregat/MetOp as presented here, the main purpose was to identify the correlation between the Fregat burns performance, being out of ground station visibility, and the antenna angles at the ground station.

As a major result from the visibility analysis Kerguelen could be identified as ground station which should acquire the spacecraft under all analysed contingency cases. The values of antenna angles provided by the stations to Flight Dynamics at specific times together with acquisition and loss of signal times could provide a good initial guess of the performance error of the Fregat burn. This information could be used to select a TOV for the next station. It was shown that most of the subsequent ground station have a good chance of acquiring the satellite by applying time offset values and starting searches at the right time. However each ground station shows a different sensitivity which on one hand allows to distinguish between the different contingency cases but on the other hand shows the necessity of a proper analysis in advance to be able to react properly under time pressure and to include the most valuable ground stations into the operations. Otherwise acquisition opportunities are lost.

Of course such an analysis needs to be wished and financed by the project. However if one compares the necessary effort with the improvement of acquiring the satellite in potential contingency cases this certainly pays off. Therefore it is expected that similar studies will be performed for future launches.

7. REFERENCES

1. Ziegler, G., *ESA/ESOC First Acquisition Strategies*, Proceedings of 17th ISSFD, Moscow, Russia 2003.